

An Unstructured Mesh Generation Algorithm for Shallow Water Modeling

SCOTT C. HAGEN^{a,*}, OLAF HORSTMANN^b and ROBERT J. BENNETT^c

^aUniversity of Central Florida, Orlando, FL 32816-2450, USA; ^bBrandenburg University of Technology, Karl-Marx-Strasse 17, D-03044 Cottbus, Germany; ^cMarshall, Provost and Associates, 340 North Causeway, New Smyrna Beach, FL 32169, USA

The successful implementation of a finite element model for computing shallow water flow requires: (1) continuity and momentum equations to describe the physics of the flow, (2) boundary conditions, (3) a discrete surface water region, and (4) an algebraic form of the shallow water equations and boundary conditions. Although steps (1), (2), and (4) may be documented and can be duplicated by multiple scientific investigators, the actual spatial discretization of the domain, i.e. unstructured mesh generation, is not a reproducible process at present. This inability to automatically produce variably-graded meshes that are reliable and efficient hinders fast application of the finite element method to surface water regions.

In this paper we present a reproducible approach for generating unstructured, triangular meshes, which combines a hierarchical technique with a localized truncation error analysis as a means to incorporate flow variables and their derivatives. The result is a process that lays the groundwork for the automatic production of finite element meshes that can be used to model shallow water flow accurately and efficiently. The methodology described herein can also be transferred to other modeling applications.

Keywords: Unstructured mesh; Finite element; Hierarchical; Truncation error; Shallow water model

1. INTRODUCTION

Recent advances in surface water modeling have permitted the development and successful implementation of coastal ocean circulation models for increasingly larger domains (Lynch, 1983; Kinnmark, 1984; Westerink and Gray, 1991; Luettich *et al.*, 1992; Blain *et al.*, 1994; Westerink *et al.*, 1994; Kolar *et al.*, 1996). While a large domain increases the predictive capabilities of coastal ocean models (Blain *et al.*, 1994; Westerink *et al.*, 1994), it complicates the process of computational node placement. Large domains require a strategic placement of nodes in order to maintain acceptable levels of local and global accuracy for a given computational cost. However, the actual gridding of larger, more complex domains relies on crude criteria and results in a mesh that is user-dependent and indirectly related to the physics of flow. In the following, the process of boundary definition and computational node placement will be discussed and an automatizable method of mesh generation will be presented that more successfully couples the physics, as represented by discrete equations, underlying tidal flow and circulation to the mesh generation process.

Larger domains warrant a method of gridding that utilizes unstructured meshes, e.g. the finite element method, which allows for spatially-varying levels of discretization. Since, in general, shallower water has a higher localized wave number content than deeper water, higher resolution will be required in shallow water regions. Furthermore it has been shown that the computed response is highly sensitive to grid resolution in regions with steep bathymetric gradients (Westerink *et al.*, 1992; Luettich and Westerink, 1995; Hagen, 1998; Hagen *et al.*, 2000; 2001). Two-dimensional (2D) response structures associated with intricate shorelines, 2D topography, amphidromes (the intersection of all phase lines and a point at which all cotidal lines meet) and resonant bays also require local refinement of grids. Conversely, deep ocean waters usually result in large expanses with more slowly varying response structures in space, which can utilize a coarser level of resolution. These considerations indicate that variably-graded meshes are needed, which, once they are generated, are easily implemented with the finite element method.

The method of production of variably-graded meshes for large-scale domains is currently poorly defined,

*Corresponding author. E-mail: shagen@mail.ucf.edu

imprecise and *ad hoc*. It is a tedious and time-consuming process at best. Since no robust criterion or node spacing routine exists that incorporates the aforementioned physical characteristics and subsequent responses into the mesh generation process, modelers are left to rely on their knowledge of particular domains and their intuition. While there has been progress made in the automatic production of unstructured meshes for coastal and ocean circulation modeling (Frey, 1987; Ho-Le, 1988; Jones and Richards, 1992; Kashiyama and Okada, 1992; Taniguchi *et al.*, 1992; Turner and Baptista, 1993; Henry and Walters, 1995), the process as currently practiced is far from automatic. As a result, one modeler cannot replicate another's results unless they possess the original mesh. Further, the fast application of the finite element method to un-gridded surface water regions is not possible.

We utilize a localized truncation error analysis (LTEA), an *a posteriori* error estimation procedure, to define local limits on element sizes and then interpret these requirements with a hierarchical technique. The LTEA is of the actual discrete equations and includes approximations to the variables being simulated and their derivatives (Hagen, 1998; Hagen *et al.*, 2000; 2001). Thus our LTEA-based approach directly couples the estimated truncation errors to the actual mesh generation process. We present our progress toward an automatic procedure by describing an example mesh generation for the entire coast of South Carolina.

2. SOUTH CAROLINA MODEL

2.1 South Carolina Coastal Domain

The objective of this paper is to demonstrate that 2D, finite element meshes that will deliver accurate and efficient solutions can be automatically produced. We choose the

coastal region of South Carolina (Fig. 1) because it provides an illustrative example for our mesh generation procedure. In addition, a mesh is needed to generate a tide stage hydrograph at the downstream end of the Waccamaw River for the National Weather Service's Southeast River Forecast Center.

The project area is located in the northern region of the South Atlantic Bight along the southeast coast of the United States. The Waccamaw River drains the coastal areas of southern North Carolina and northern South Carolina. The river leaves Lake Waccamaw in North Carolina and flows southward through Conway, South Carolina. From there, the river flows southward to the confluence with the Great Pee Dee and Black Rivers, through Winyah Bay, and into the Atlantic Ocean as shown in Fig. 1.

For the purposes of the present paper and the tidal study, a grid domain for the area surrounding the Waccamaw River coastal region is defined. The domain is chosen to be large enough to include the area surrounding Charleston, South Carolina where historical tidal stage data is available. Further details on boundary definition, bathymetry and the entire finite element mesh generation approach will be provided in "Mesh generation".

2.2 Finite Element Model

The computations that are performed to generate a 2D LTEA-based grid for the South Carolina domain are realized with a finite element model of the linearized shallow water equations. There are two main reasons that justify using a linear form of the shallow water equations. First, the concept of mesh generation that is based on multiple orders of the truncation error series is in the early stages of research. Simplicity, here in the form of linearized shallow water equations, facilitates a clear understanding of the details and implications of this

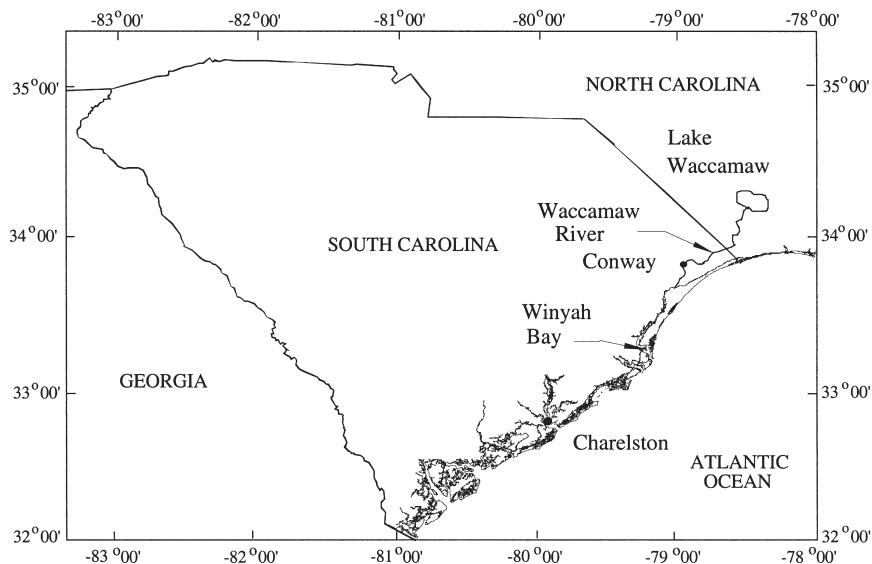


FIGURE 1 The coast of South Carolina.

theory. Second, shallow water modeling of a long-wave process in a large basin is weakly nonlinear. Because the nonlinear-term contribution is minimal, examination of the truncation error associated with the linear form of the shallow water equations should produce a finite element grid that will be suited for nonlinear simulations.

2D shallow water equations are comprised of depth-integrated formulations of primitive continuity and momentum equations. For this paper, the continuity equation is formulated in the generalized wave continuity equation form (GWCE) (Kinnmark, 1984; Luetlich, *et al.*, 1992). The linearized 2D GWCE is given by

$$\frac{\partial^2 \eta}{\partial t^2} + \tau_0 \frac{\partial \eta}{\partial t} - g \left[\frac{\partial}{\partial x} \left(h \frac{\partial \eta}{\partial x} \right) - \frac{\partial}{\partial y} \left(h \frac{\partial \eta}{\partial y} \right) \right] - (\tau - \tau_0) \left[\frac{\partial}{\partial x} (uh) - \frac{\partial}{\partial y} (vh) \right] = 0 \quad (1)$$

and the 2D, linearized, non-conservative momentum equations are expressed as

$$\frac{\partial u}{\partial t} + g \frac{\partial \eta}{\partial x} + \tau u = 0 \quad (2)$$

$$\frac{\partial v}{\partial t} + g \frac{\partial \eta}{\partial y} + \tau v = 0 \quad (3)$$

where t is the time, x and y the spatial coordinates, η the deviation of the free surface from the geoid, u the velocity in the x -direction, v the velocity in the y -direction, τ_0 a weighting parameter in the GWCE, which controls the contribution from primitive continuity, g the gravitational acceleration, h the depth below the geoid and τ is the bottom friction coefficient.

3. MESH GENERATION

The following sub-sections describe five major tasks that are performed to produce an unstructured mesh for the South Carolina model domain. First, a discrete boundary is defined such that a user-defined level of detail is met. Second, a structured grid is produced to serve as a base grid that contains all domain dependent detail (e.g. bathymetry). Third, point-wise, time-independent truncation errors are analyzed at the nodes of the base grid from harmonic, linear simulation results. Fourth, local element sizes are produced in the form of maximum allowable radii. Finally, a hierarchical technique is employed to generate a variably graded mesh that follows the maximum allowable radii requirements on element sizes. The result is a process that lays the groundwork for the automatic production of finite element meshes that can be used to model shallow water flow accurately and efficiently.

3.1 Boundary Definition

World Vector Shoreline data is downloaded from the United States Geologic Survey Coastal Data Information

TABLE I End points of three segments for the Waccamaw River (see Fig. 2)

Longitude (degrees west)	Latitude (degrees north)
79.247929	33.353808
79.100298	33.522266
79.142248	33.500265
79.247635	33.395684
79.242502	33.432060
79.279098	33.352561

Internet site at <http://crusty.er.usgs.gov/coast/getcoast.html>. Shoreline data with a coarse resolution of 1:250,000 (1:250) is extracted for the area bounded by 32 and 34° north latitude and 78 and 81.5° west longitude (see Fig. 1). This corresponds to the entire shoreline of the South Carolina Coast plus a small section of the North Carolina coast up to Cape Fear. The data consists of nodes (longitude and latitude locations) that demarcate land/ocean boundaries.

Since the boundaries for the 1:250 resolution do not extend far enough into the estuary where the final tide stage hydrograph is desired, three segments of 1:70,000 (1:70) resolution data for the Waccamaw River are extracted to create a shoreline for this region. Table I provides the end points of each these segments. The 1:70 data is used to illustrate an algorithm for boundary node definition.

Figure 2(a) displays the raw shoreline data with the 1:70 resolution for the Waccamaw River boundary. Since the total number of nodes/elements in the finite element grid is a function of the boundary node resolution, the number of nodes on the boundary is minimized while maintaining physical geometry characteristics. In addition, the spacings between the nodes are required to be relatively uniform to assure that the triangular elements formed adjacent to the boundary nodes are approximately equilateral.

To accomplish both objectives, a minimum/maximum spacing routine is implemented. The routine deletes nodes that are closer together than a specified minimum distance and adds a node(s) when the spacing between two nodes is greater than 1.75 times the minimum spacing distance. A minimum distance of 0.002° is chosen for this region of the grid domain. In addition, all tributaries with a width of less than 0.002° are deleted. The final shoreline for the Waccamaw River boundary is displayed in Fig. 2(b).

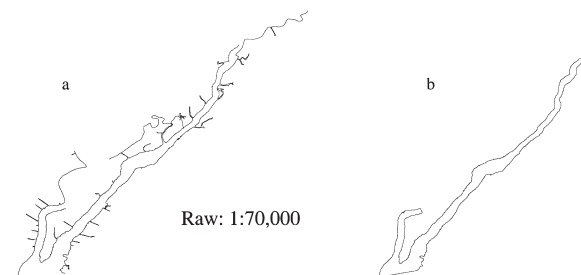


FIGURE 2 Waccamaw River boundary: (a) raw data, (b) refined.

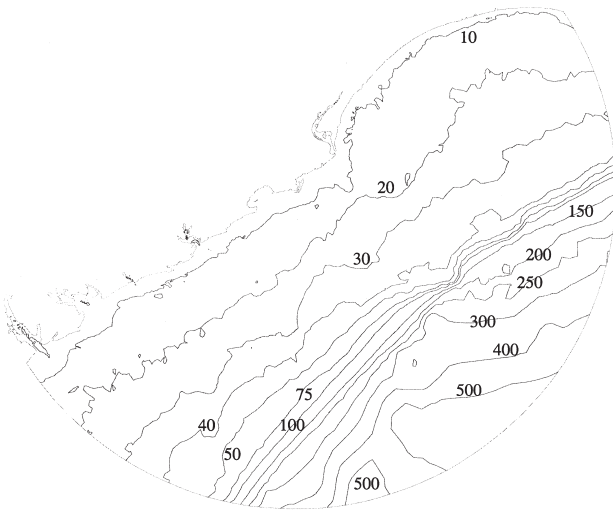


FIGURE 3 South Carolina domain boundary with depth contours (in m).

The minimum/maximum spacing routine is also applied to the 1:250 resolution data. Here an arbitrary minimum spacing of 0.005° is utilized. The refined Waccamaw River boundary is then incorporated. Finally, an ocean boundary is generated by swinging an arc of node points. The center between the two end land boundary points is established at 79.38335° west, 33.02820° north and an ocean boundary node is placed at intervals equal to an arc length of 0.00834° . The final boundary is presented in Fig. 3. Depth contours, from the National Geophysical Data Center Coastal Relief Model (1999), are also included in Fig. 3.

3.2 Structured Grid

The next step is to generate a structured grid. This is done in our application using polar coordinates. First, a center is established at 79.38335° west, 33.02820° north. (Note, this is the same location as is used for defining the ocean boundary.) Second, 198 arcs are swung beginning at 135° and ending before a complete revolution is made. Each arc radius, r , is incremented by $dr = 1.59031^\circ/199$, where 1.59031° is the distance from the center to the sea boundary. A node is placed every $d\theta = dr/r$ as each arc is swung.

In addition, nodes are placed within the Waccamaw River boundary (Fig. 2). After the initial nodes from the previous routine are removed from within the Waccamaw River boundary, a center is established at 79.253024° west, 33.352297° north. Here 73 arcs are swung beginning at 45° and ending at 135° . Each arc radius, r , is incremented by $dr = 0.1931736^\circ/74$. A node is placed every $d\theta = dr/r$ as each arc is swung. All boundary and interior nodes are then triangulated and bathymetry from the National Geophysical Data Center Coastal Relief Model (1999) is interpolated at each node point to complete a *structured* mesh with a total of 69,816 nodes.

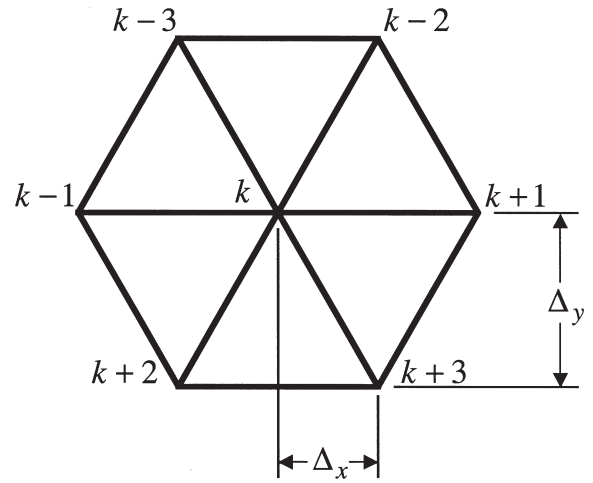


FIGURE 4 An interior node, k , and the surrounding nodes for a six-element configuration.

3.3 Localized Truncation Error Analysis

LTEA Formulation

The development of truncation error associated with solutions from any given structured or unstructured grid would result in a set of equations that would be tedious to work with because of the potential irregularity of the grid spacing. More importantly, the resulting equations would not lend themselves to an algorithm that promotes a domain-wide, constant truncation error, which is the basis for adjusting the local spacing. Herein, point-wise, time-independent, truncation error associated with a linear, harmonic form of the primitive momentum Eqs. (2) and (3), is developed and estimated for the central node of an assumed regular triangular mesh (Fig. 4).

It is assumed that the finite element mesh that will be generated will have equilateral, triangular elements on a local scale (as represented by Fig. 4). The assumption permits: (1) an *a priori* estimation of truncation error for the finite element mesh that is being developed; (2) that Δ_y may be expressed as a function of Δ_x , i.e. $\Delta_y = \sqrt{3}\Delta_x$.

Note that the assumption of equilateral triangular elements would be valid locally throughout a given finite element mesh, however, since the meshes that are generated will have irregular spacings, the assumption cannot be valid globally. This does lead to some dependence on *pseudo* 2D mesh generation because the mesh design is constrained to use equilateral triangles.

Because the truncation error is developed for a specific configuration, a valence of six (Fig. 4), the truncation error series may be summed, truncated and solved together for Δ , noting that $\Delta = \Delta_x$. This provides an estimation of the second and fourth-orders of truncation error associated with the discrete form of the second and fourth-orders of truncation error associated with the discrete form of the linear, harmonic, non-conservative momentum Eqs. (2) and (3), on the interior nodes of an equilateral triangular

grid (Hagen, 1998)

$$\begin{aligned}
\tau_{ME} = & \Delta^2 \left[\left(\frac{i\varpi + \tau}{2} \right) \left(\frac{\partial^2 \hat{u}_k}{\partial x^2} + \frac{\partial^2 \hat{v}_k}{\partial x^2} + \frac{\partial^2 \hat{u}_k}{\partial y^2} + \frac{\partial^2 \hat{v}_k}{\partial y^2} \right) \right. \\
& \left. + \frac{g}{2} \left(\frac{\partial^3 \hat{\eta}_k}{\partial x^3} + \frac{\partial^3 \hat{\eta}_k}{\partial x^2 \partial y} + \frac{\partial^3 \hat{\eta}_k}{\partial x \partial y^2} + \frac{\partial^3 \hat{\eta}_k}{\partial y^3} \right) \right] \\
& + \Delta^4 \left[\left(\frac{i\varpi + \tau}{8} \right) \left(\frac{\partial^4 \hat{u}_k}{\partial x^4} + \frac{\partial^4 \hat{v}_k}{\partial x^4} + 2 \frac{\partial^4 \hat{u}_k}{\partial x^2 \partial y^2} \right) \right. \\
& \left. + 2 \frac{\partial^4 \hat{v}_k}{\partial x^2 \partial y^2} + \frac{\partial^4 \hat{u}_k}{\partial y^4} + \frac{\partial^4 \hat{v}_k}{\partial y^4} \right] \\
& + \frac{g}{24} \left(\frac{22 \partial^5 \hat{\eta}_k}{10 \partial x^5} + \frac{\partial^5 \hat{\eta}_k}{\partial x^4 \partial y} + 2 \frac{\partial^5 \hat{\eta}_k}{\partial x^3 \partial y^2} \right. \\
& \left. + 6 \frac{\partial^5 \hat{\eta}_k}{\partial x^2 \partial y^3} + 3 \frac{\partial^5 \hat{\eta}_k}{\partial x \partial y^4} + \frac{9 \partial^5 \hat{\eta}_k}{5 \partial y^5} \right) \quad (4)
\end{aligned}$$

where \hat{u} , \hat{v} and $\hat{\eta}$ are the complex amplitudes of u , v and η evaluated at node k (the center node in Fig. 4), g the gravitational acceleration, τ the bottom friction coefficient, $i = \sqrt{-1}$, and ϖ is the response frequency.

Central difference approximations for a regular finite difference grid ($dx = dy$) are applied to estimate the partial derivatives of Eq. (4). These approximations are carefully developed such that the estimate of the second and third-order partial derivatives have a leading order accuracy of order four and the estimate of the fourth and fifth-order partial derivatives have a leading-order accuracy of order two (Hagen, 1998).

LTEA Computations

Hydrodynamic calculations are performed with ADCIRC-2DDI, a 2D depth integrated circulation code (Luettich *et al.*, 1992). The simulation utilizes linear, Galerkin finite elements in two dimensions, with triangular elements, and employs a constant bottom friction coefficient and GWCE weighting parameter of 0.0004. A no-flow boundary condition is enforced at all land boundaries and open ocean boundaries are forced with the M_2 tidal constituent. Thirty days of real time are simulated with the structured grid, which is described in ‘‘Structural grid’’, to ensure that a dynamic steady-state is achieved. A time step of 30 s is used. In addition, a hyperbolic ramping function (Luettich *et al.*, 1992) is imposed during the first two days. Harmonic solutions from the structured grid simulation are employed to evaluate Eq. (4), with $\Delta = 900$ m, which is the approximate spacing between nodes for the structured grid, and produce local truncation error estimates.

3.4 Maximum Allowable Radii

A scalar value, which represents a radius of maximum allowable node spacing, is computed at interior nodes of the structured grid by setting Eq. (4) equal to the peak local truncation error value associated with the structured grid, $7.90 \times 10^{-6} \text{ m/s}^2$. This complex quadratic is solved for Δ with the minimum real root selected as the scalar value (Hagen, 1998). The scalar value represents a radius of maximum allowable node spacing. This procedure is carried out for interior nodes of the structured grid.

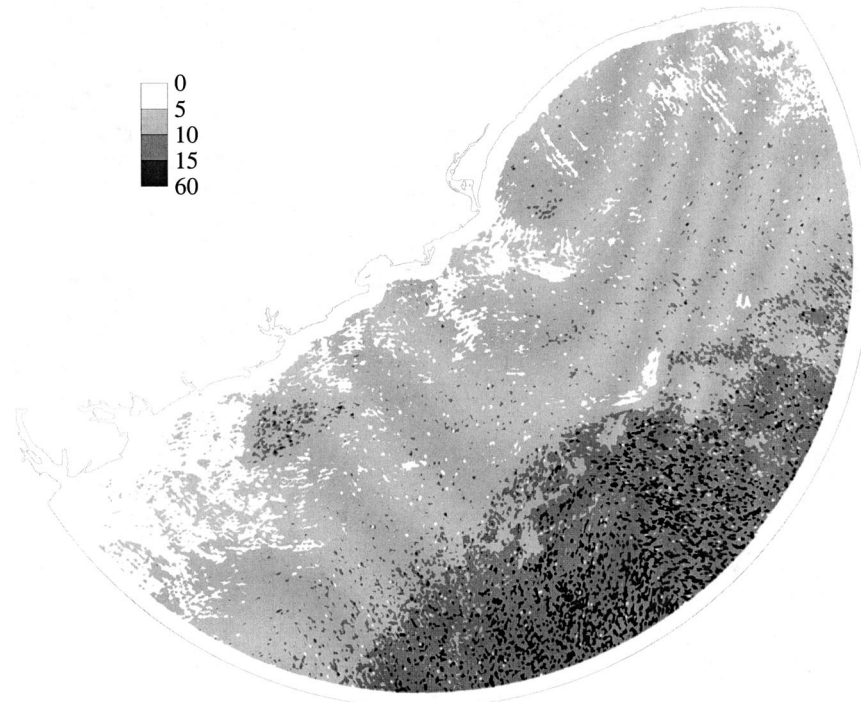


FIGURE 5 Maximum allowable radii (in kms).

Figure 5 presents a contour plot of the maximum allowable radii for the South Carolina domain. Note that use of the central difference approximations does not permit an estimate of the local truncation error up to the boundaries. The local node spacing requirements are changed as a result of forcing the truncation error to be constant, with the one exception being the node where the peak local truncation error is attained. Maximum allowable radii range from 0.9 to 55.89 km.

3.5 Unstructured Mesh Generation Based on the SHIDOMO Approach

A mesh generation method based upon the concept of schematized hierarchical domain models (SHIDOMO) is employed to automatically produce an unstructured mesh (Horstmann, 1998). The maximum allowable radii from the “Maximum allowable radii” section are utilized.

For the mesh of the South Carolina coast area it is crucial to preserve the structure of the coastline and the discrete representation of shore and nearshore features, such as the Waccamaw River and other estuaries in addition to islands situated near the shore. Therefore, the following features are isolated for the input to the SHIDOMO process:

- South Carolina Coastline and sea-side boundary (as defined in the structured grid);
- internal terrain near the shore (where no modification of the mesh will occur);
- internal terrain offshore (rest of the domain).

The different features are extracted from the structured grid (described in “Structured grid”) to obtain polygonal definitions and digital terrain models for the linear and planar features, respectively.

The actual adaptive step in the SHIDOMO process is the extraction of segments during traversing of the hierarchical domain models for the different domain features. Every single segment met during the traversing may in principle be examined in terms of its own

properties (size, shape, physical value representation), its relative position towards a target entity (polygon, etc.) or the properties of a reference entity at its position. In general, the application of various adaptation criteria is possible through a generic interface.

A background mesh approach is employed for the production of the South Carolina mesh, which allows for a quite simple algorithmic handling of the problem. The structured grid from “Structured grid”, with the allowable maximum radii stored at its nodes, is loaded into the background as a control space. To make a decision about the fitness of a segment to be incorporated into the adaptive selection, its size is simply compared to the allowable size, that can be interpolated from the background mesh at a simplex’ center position (Fig. 6).

The following eight steps are performed to produce the South Carolina mesh.

1. The trend of the maximum allowable radii is extrapolated into the regions near the boundaries, where no LTEA spacing calculations can be performed.
2. For the seaside boundary a hierarchical domain is set up with a minimum resolution of about 300 m (minimum linear segment length).
3. From this model, an adaptive segmentation is selected with the target segment lengths determined by interpolation of the allowable spacing from the structured background grid at the intersection of the segments middle perpendicular with the background meshes boundary. The segmentation is transformed into an adapted boundary polygon.
4. The adapted seaside boundary is merged with the unchanged shore boundary polygon, which has been extracted from the structured grid.
5. A hierarchical domain model is set up for the offshore terrain with a maximum resolution of 300 m (triangular segment side length). The adaptive set of segments is selected from that model by traversing the tree and comparing each segments side length to the allowable spacing for the segments center position defined in the background mesh.

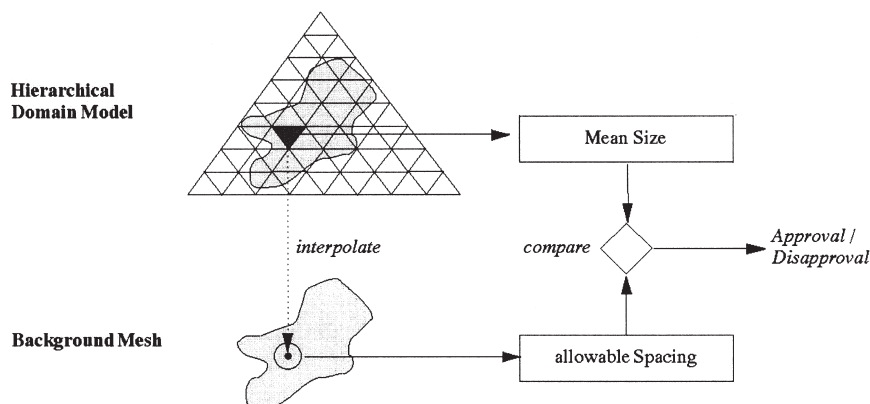


FIGURE 6 Background mesh technique.

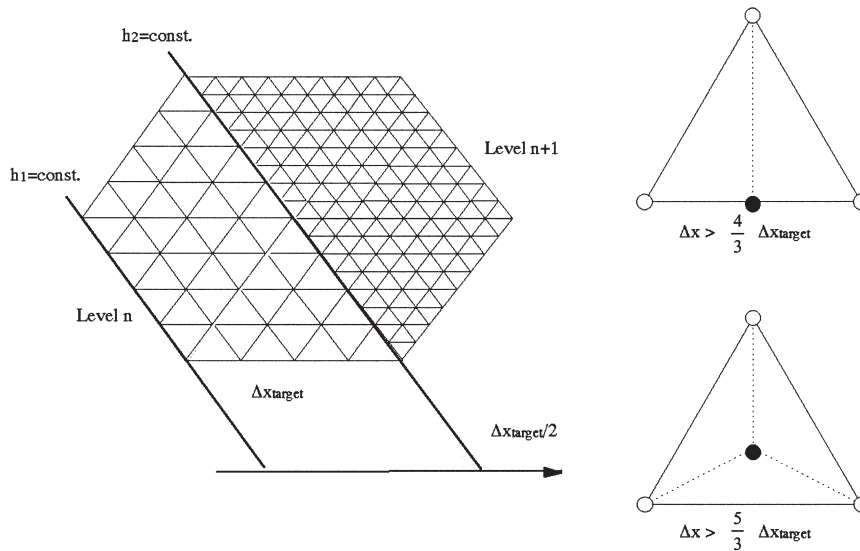


FIGURE 7 Mesh grading.

6. From this adaptive segment set, a set of internal nodes is generated. This is merged with the set of internal nodes from the nearshore boundary strip extracted from the structured grid.
7. The resulting set of internal nodes is merged with the boundary polygon obtained from step 4.
8. The resulting set of internal nodes and boundary edges is triangulated with a Delaunay triangulation method.

One major problem of the multi-scale representation of domain features, with geometrical and physical properties in a hierarchical tree order, is that the scale resolution is not continuous but discrete. This always yields size steps of two in adaptive meshes produced with the SHIDOMO approach (just as in bintree/quadtree methods, which the SHIDOMO meshing approach resembles not conceptually, but in its final effects). This property is shown in Fig. 7. If the adaptation rule cumulates in a decision of the form (in *pseudo-code*):

```

if (delta_xseg < delta_xtarget(x,y))
    choose_segmet;
else
    try_children;

```

then at a “target size iso line” h_1 in the domain the size of the segments of level n will be fitting perfectly, while at iso line h_2 the segments of level $n + 1$ will fit perfectly and a level step will be provoked there. But between lines h_1 and h_2 from Fig. 7 the segments will be too large, reaching the double required size at iso line h_2 , if the behavior of Δx_{target} is continuously changing in the domain (x,y) as suggested in the sketch and as will be the usual case in practical applications. This may cause a rather poor mapping of the adaptation requirements into the mesh.

To improve the situation, additional measures are taken to enhance the grading of the quadtree-like portion of the unstructured South Carolina mesh. These measures affect

the transformation of segments into respective simplexes after compilation of the adaptive meshes. Three nodes from each triangular segment (one for each corner) are generated in the transformation process to determine the internal node distribution in the final mesh. To refine the mesh size grading, an additional node is generated on one of the sides of the segment if its size is greater then $4/3$ times the target size, by dividing the segment in two. A node is generated in the center of the segment if the segment size is more than $5/3$ of the required size, by dividing it in three (Fig. 7).

There is a jump in resolution from the fine structured grid to that of the LTEA-based portion of the grid. (Note from Fig. 5 that maximum allowable radii are not computed up to the coastal boundary). Therefore, a transition zone is established around the seam between both mesh portions. A scaling factor of 0.65 is applied to the maximum allowable radii during the SHIDOMO selection procedure to produce an area with a resolution halfway between the intended LTEA-based resolution and the nearshore resolution.

The unstructured mesh obtained from the SHIDOMO procedure has a controlled quality in terms of element shapes and mesh resolution adaptation. Degenerated elements are widely avoided (although some may occur in unfortunate cases even with adapted boundaries) and the method promotes a dominance of very well shaped (i.e. equilateral) triangles in the mesh. However, to improve the mesh element overall shape quality, mainly in the size transition zones, some smoothing is employed. In this pilot implementation a simple Laplacian smoothing algorithm is utilized for this task.

Figure 8 displays the resulting mesh. The final unstructured mesh is reduced to 10,013 nodes from the 69,816 nodes of the structured mesh. All algorithms described herein for the generation of the unstructured mesh, which include a discrete boundary definition and a high-resolution of bathymetric features (through the

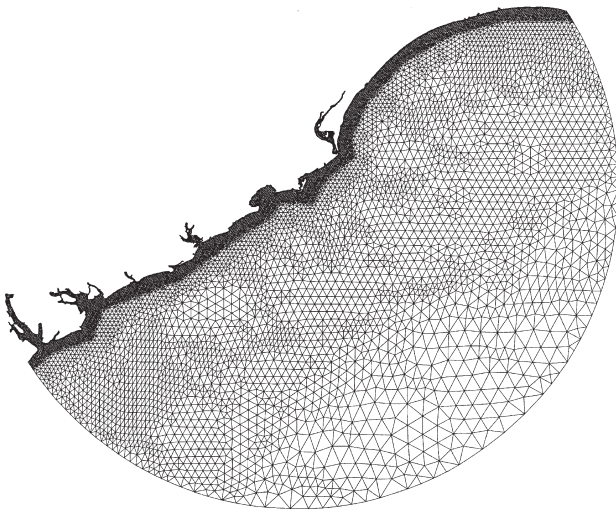


FIGURE 8 Unstructured mesh for the South Carolina domain.

structured grid), lead toward a fully automatic procedure. The LTEA-based approach to a variably graded mesh assimilates those bathymetric features from the structured grid that are important to the physics of shallow water flow, as represented by discrete equations, by maintaining refinement of the mesh where high gradients in the response variables dictate and allowing relaxation of element sizes elsewhere. The modeler need only define the limits of the boundary and specify a minimum element size for the structured grid. It is noted that the procedure as presently defined is limited by the central difference approximations of partial derivatives in the truncation error series, which do not permit an estimation of truncation error up to the boundary.

4. SIMULATIONS

Fully nonlinear, hydrodynamic calculations are performed with ADCIRC-2DDI, a 2D integrated circulation code (Luettich *et al.*, 1992). The simulation employs a constant bottom friction coefficient of 0.003, a GWCE weighting parameter of 0.009 and an eddy viscosity of 0.0. A no-flow boundary condition is enforced at all land boundaries and open ocean boundaries are forced with the M_2 , M_4 , M_6 , O_1 , N_2 , S_2 , K_1 , and *STEADY* tidal constituents. 90 days of real time are simulated with the unstructured mesh (Fig. 8), beginning at 12:00 a.m. (GMT) on 1 January 1998. A time step of 10 s is used. In addition, a hyperbolic ramping function (Luettich *et al.*, 1992) is imposed during the first five days.

Figure 9 displays the historical and modeled tide elevations for a 15-day period at the end of March 1998. When comparing the modeled results to the historical data, it is important to realize that the historical data results from all actual astronomical *and* meteorological tidal forcings present at that time while the modeled results include only the astronomical tide forcings. Figure 9 indicates that the modeled results estimated the tidal elevations reasonably well at Charleston, SC.

5. CONCLUSIONS

We have shown that an unstructured mesh for coastal and ocean circulation modeling can be automatically produced, by combining the results from a LTEA and a schematized hierarchical domain model. The truncation error-based approach to generating local node spacing requirements incorporates an *a posteriori* estimation of

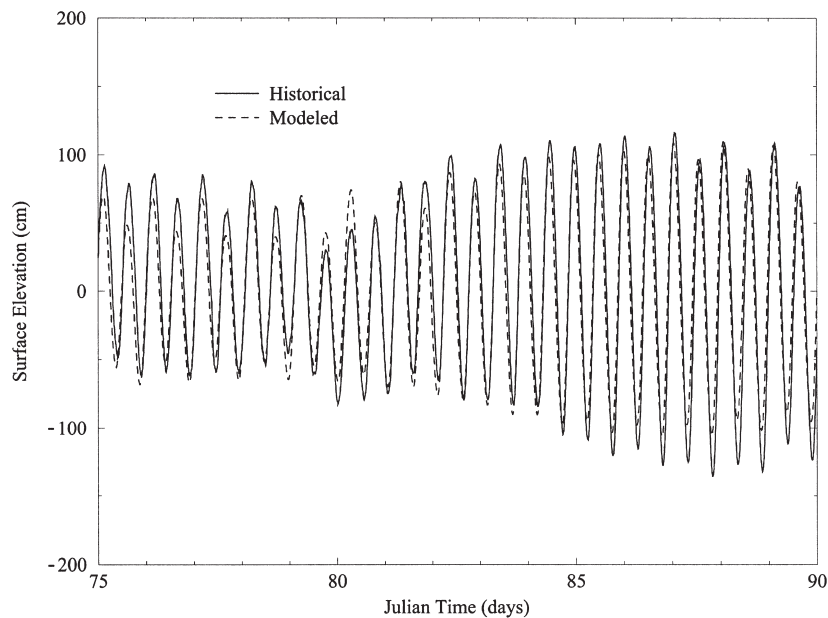


FIGURE 9 Charleston historical data and modeled results, 16 March 1998–31 March 1998.

flow variables and their derivatives, which enable the resulting mesh to model shallow water flow accurately and efficiently. The hierarchical technique permits the mesh to be generated in a reproducible fashion. The ability to assimilate a large bathymetric data set into a variably graded mesh provides a further benefit of the procedure. The end result is a process that will permit the fast application of the finite element method to new shallow water modeling challenges.

While the LTEA-based process lays the groundwork for fully automatic production of finite element meshes, refinements must occur before a generalized application is produced. At present, central difference approximations are used to estimate partial derivatives in the truncation error series. As a result, local truncation error can only be estimated on the main interior for an existing structured grid. A different technique must be developed that will permit truncation error estimation, and thereby maximum allowable radii computations, to be carried out up to and including the boundary, which will have the added benefit of incorporating the effect that the physics of flow has on boundary definition. In addition, the mesh generation algorithms of a LTEA should be extended to include nonlinear bottom friction, Coriolis terms, tidal potential terms, and multiple tidal constituents.

The LTEA-based procedure may also enhance shallow water modeling problems that require adaptive mesh refinement, e.g., storm surge simulations and transport problems. The process results in a variably graded mesh that can be used as a base grid for any adaptive mesh refinement scheme. In addition, further refinements in the procedure, as noted above, may lead to an adaptive mesh refinement process that is LTEA-based. The methodology described herein can also be transferred to other modeling applications.

Acknowledgements

This paper is funded in part from University Cooperation for Atmospheric Research Subaward No. UCAR S98-98908 pursuant to National Oceanic and Atmospheric Administration Award No. NA67WD0097. The views expressed herein are those of the author(s) and do not necessarily reflect the views of NOAA, its sub-agencies, or UCAR.

References

- Blain, C.A., Westerink, J.J. and Luettich, Jr., R.A. (1994) "The influence of domain size on the response characteristics of a hurricane storm surge model", *J. Geophys. Res.* **99**(C9), 18467–18479.
- Frey, W.H. (1987) "Selective refinement: a new strategy for automatic node placement in graded triangular meshes", *Int. J. Numer. Meth. Fluids* **24**, 2183–2200.
- Hagen, S.C., Finite element grids based on a localized truncation error analysis PhD Dissertation (Department of Civil Engineering and Geological Sciences, University of Notre Dame, IN).
- Hagen, S.C., Westerink, J.J. and Kolar, R.L. (2000) "One-dimensional finite element grids based on a localized truncation error analysis", *Int. J. Numer. Meth. Fluids* **32**, 241–261.
- Hagen, S.C., Westerink, J.J., Kolar, R.L. and Horstman, O. (2001) "Two dimensional, unstructured mesh generation for shallow water models: comparing a wavelength-based approach to a localized truncation error analysis", *Int. J. Numer. Meth. Fluids* **35**, 669–686.
- Henry, R.F. and Walters, R.A. (1995) "Geometrically based, automatic generator for irregular triangular networks", *Comm. Numer. Meth. Engr.* **9**, 555–566.
- Ho-Le, K. (1988) "Finite element mesh generation methods: a review and classification", *Comput.-Aided Engng. J.* **20**, 27–38.
- Horstmann, O., (1988) "Adaptive grids for hydroengineering based upon predefined construction segments", In: Holz, K.P., *et al.* eds, *Advances in Hydro-Science and -Engineering Proceedings of the Third International Conference on Hydrosience and Engineering, Vol. III.*
- Jones, N.L. and Richards, D.R. (1992) "Mesh generation for estuarine flow modeling", *J. Wat., Port, Coast., Ocean. Engng.* **118**, 599–614.
- Kashiyama, K. and Okada, T. (1992) "Automatic mesh generation method for shallow water flow analysis", *Int. J. Numer. Meth. Fluids* **15**, 1037–1057.
- Kinnmark, P.E., The shallow water wave equations: formulation, analysis and application PhD Dissertation (Department of Civil Engineering, Princeton University, NJ).
- Kolar, R.L., Gray, W.G. and Westerink, J.J. (1996) "Boundary conditions in shallow water models—an alternative implementation for finite element codes", *Int. J. Numer. Meth. Fluids* **22**, 603–618.
- Luettich, Jr., R.A. and Westerink, J.J. (1995) "Continental shelf scale convergence studies with a barotropic tidal model", In: Lynch, D.R. and Davies, A.M., eds, *Quantitative Skill Assessment for Coastal Ocean Models AGU, Vol. 47*, pp 349–371.
- Luettich Jr., R.A., Westerink, J.J., Scheffner, N.W., (1992). "ADCIRC an advanced three-dimensional circulation model for shelves, coasts and estuaries, Report 1: theory and methodology of ADCIRC-2DDI and ADCIRC-3DL". Technical Report DRP-92-6, Department of the Army.
- Lynch, D.R. (1983) "Progress in hydrodynamic modeling, review of US contributions, 1979–1982", *Rev. Geophys. Space Phys.* **21**, 741–754.
- National Geophysical Data Center Coastal Relief Model, Vol. 02 version 1.0, 1999. US South East Atlantic Coast, Boulder, CO.
- Taniguchi, T., Holz, K-P. and Ohta, C. (1992) "Grid generation for 2D flow problems", *Int. J. Numer. Meth. fluids* **15**, 985–997.
- Turner, P.J., Baptista, A.M., (1993). "Software for semi-automatic generation of two-dimensional finite element grids". *ACE/gredit Users Manual.*
- Westerink, J.J. and Gray, W.G. (1991) "Progress in surface water modeling", *Rev. Geophys.* **29**, 210–217.
- Westerink, J.J., Muccino, J.C., Luettich, Jr., R.A., *et al.* (1992) "Resolution requirements for a tidal model of the Western North Atlantic and Gulf of Mexico", In: Russell, T.F., ed, *Proceedings of the IX International Conference on Computational Methods in Water Resources.*
- Westerink, J.J., Luettich, Jr., R.A. and Muccino, J.C. (1994) "Modeling tide in the western north Atlantic using unstructured graded grids", *Tellus* **46A**, 178–199.

Copyright of International Journal of Computational Fluid Dynamics is the property of Taylor & Francis Ltd and its content may not be copied or emailed to multiple sites or posted to a listserv without the copyright holder's express written permission. However, users may print, download, or email articles for individual use.